

# Characterization of the translocon of the outer envelope of chloroplasts

Enrico Schleiff,<sup>1</sup> Jürgen Soll,<sup>1</sup> Michael Küchler,<sup>1</sup> Werner Kühlbrandt,<sup>2</sup> and Roswitha Harrer<sup>2</sup>

<sup>1</sup>Botanisches Institut, Ludwig Maximilian Universität München, 80638 München, Germany

<sup>2</sup>Max-Planck-Institut für Biophysik, 60528 Frankfurt am Main, Germany

The protein translocon of the outer envelope of chloroplasts (Toc) consists of the core subunits Toc159, Toc75, and Toc34. To investigate the molecular structure, the core complex was purified. This core complex has an apparent molecular mass of ~500 kD and a molecular stoichiometry of 1:4:4–5 between Toc159, Toc75, and Toc34. The isolated translocon recognizes both transit sequences and precursor proteins in a GTP-dependent manner, suggesting its functional integrity. The complex is embedded by the

lipids phosphatidylcholine and digalactosyldiacylglyceride. Two-dimensional structural analysis by EM revealed roughly circular particles consistent with the formation of a stable core complex. The particles show a diameter of ~130 Å with a solid ring and a less dense interior structure. A three-dimensional map obtained by random conical tilt reconstruction of electron micrographs suggests that a “finger”-like central region separates four curved translocation channels within one complex.

## Introduction

Most chloroplast proteins are encoded by the nuclear genome and synthesized in the cytosol as preproteins with an NH<sub>2</sub>-terminal transit sequence, which is cleaved upon import (Keegstra and Cline, 1999; Schleiff and Klösgen, 2001). Heterooligomeric machineries are required for translocation of preproteins across the chloroplast membranes (Keegstra and Cline, 1999; Schleiff and Soll, 2000). So far, four different outer envelope proteins (OEPs)\* (Toc159, Toc75, Toc64, and Toc34; translocon at the outer envelope of chloroplasts [Schnell et al., 1997]) and six different proteins of the inner envelope (Tic110, Tic62, Tic55, Tic40, Tic22, and Tic20; translocon at the inner envelope of chloroplasts) are known to be involved in the translocation process (Schnell et al., 1997; Keegstra and Cline, 1999; Küchler and Soll, 2001; Küchler et al., 2002).

Toc75 is predicted to be an integral membrane protein that forms the translocation channel of the outer envelope

(Schnell et al., 1994; Hinnah et al., 1997) and interacts with Toc159 and Toc34 (Seedorf et al., 1995; Nielsen et al., 1997). Toc159 and Toc34 contain a GTP-binding domain and are thought to form receptor units for the transit sequences (Hirsch et al., 1994; Kessler et al., 1994; Perry and Keegstra, 1994; Ma et al., 1996; Akita et al., 1997; Nielsen et al., 1997; Chen et al., 2000; Sveshnikova et al., 2000b). Toc34<sub>GTP</sub> binds preproteins with high affinity (Sveshnikova et al., 2000b; Schleiff et al., 2002a). GTP hydrolysis by Toc34, which is highly stimulated by the preprotein (Jelic et al., 2002) yields a low affinity Toc34<sub>GDP</sub> receptor (Sveshnikova et al., 2000b; Schleiff et al., 2002a). GTP hydrolysis rates might be further regulated by receptor dimerization (Sun et al., 2002). The Toc34 receptor can be switched off by phosphorylation, which in turn inhibits GTP binding (Sveshnikova et al., 2000b). Toc159 represents a second nucleoside triphosphate-dependent receptor (Hirsch et al., 1994; Kessler et al., 1994). A subpopulation seems to be localized in the cytosol (Hiltbrunner et al., 2001a); however, its function in import remains elusive. Further members of the Toc159 family include Toc132, Toc120, and Toc90, which seem to be less abundant in chloroplasts (Hiltbrunner et al., 2001a). Current results suggest that these proteins have specialized functions, since none of the family members can replace Toc159 function in a mutant, *ppi2*, which contains a tDNA insertion in the gene coding for Toc159 (Bauer et al., 2000). However, the function of Toc64 remains to be established.

At the inner envelope, Tic110 is the central unit of the translocon and is involved in most events during translocation

Address correspondence to Enrico Schleiff, Botanisches Institut, LMU München, Menzinger Str. 67, 80638 München, Germany. Tel.: 49-89-17861-182. Fax: 49-89-17861-185.

E-mail: schleiff@botanik.biologie.uni-muenchen.de

\*Abbreviations used in this paper: DGDG, digalactosyldiacylglyceride; GMP-PNP, guanylyl-imidodiphosphate; MGDG, monogalactosyldiacylglyceride; NEM, *N*-ethylmaleimide; OEP, outer envelope protein; PC, phosphatidylcholine; PG, phosphatidylglycerol; preSSU, precursor form of the small subunit of RUBISCO; RUBISCO, ribulose 1,5-biphosphate carboxylase-oxygenase; Tic, translocon at the inner envelope of chloroplasts; Toc, translocon at the outer envelope of chloroplasts.

Key words: complex structure; protein translocation; complex composition; preprotein recognition; membrane complex purification

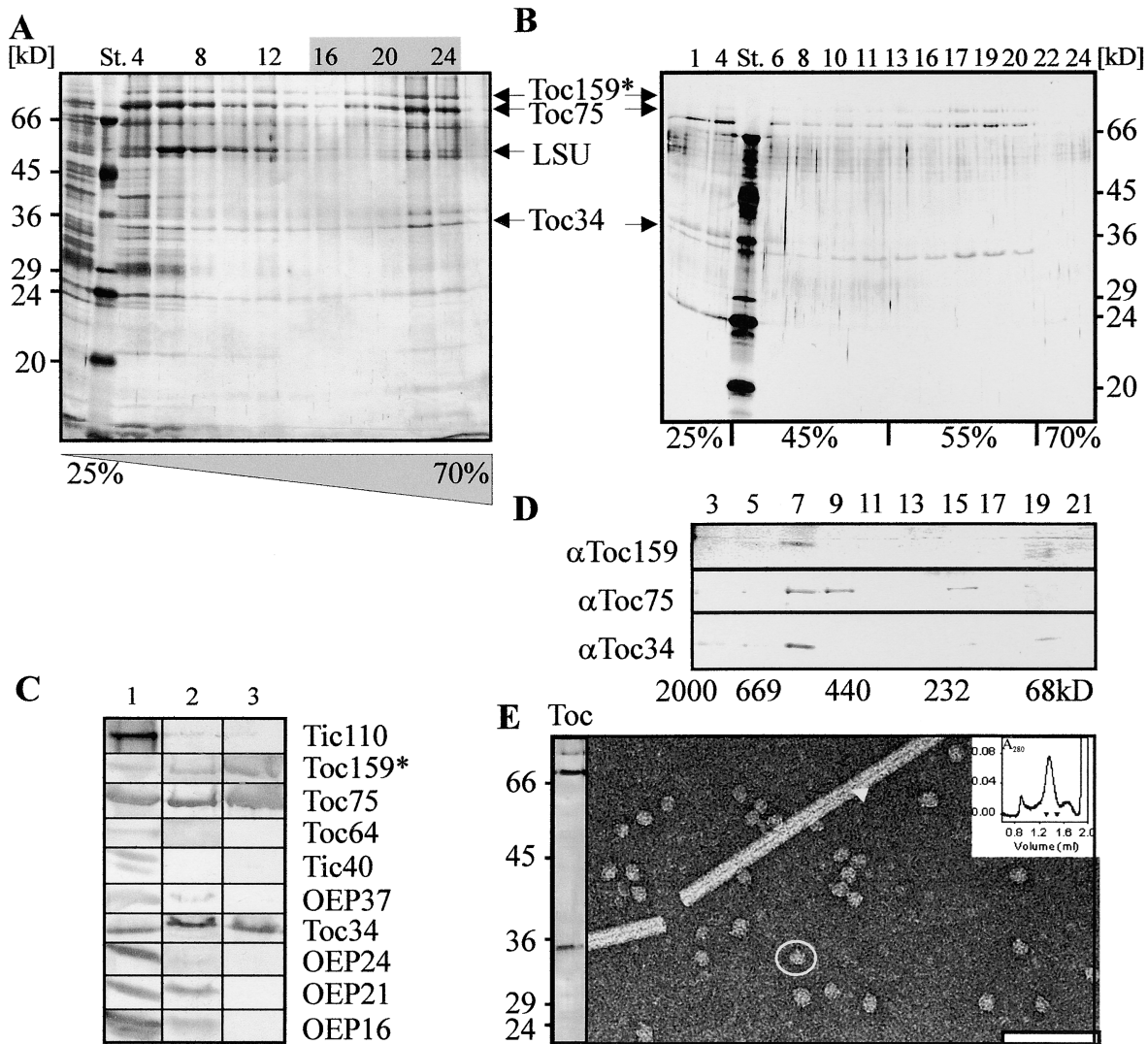


**Figure 1. The purified core complex of the chloroplast outer envelope translocon.** The outer envelope fraction was solubilized as described in Materials and methods, separated on a 25–70% sucrose density gradient (A) followed by separation of the indicated fractions (gray underlay) on a sucrose step gradient (B). A silver-stained gel of the fractions is shown. Proteins are assigned according to results of immunoblot analysis where Toc159\* indicates the 86-kD fragment of Toc159. Numbers indicate the fractions of the gradient (on top), the molecular weight (on the side), and the sucrose concentration (wt/vol; on the bottom). (C) The protein pattern of outer envelopes (lane 1), the combined fractions (gray underlay in A) of the first gradient (lane 2), or the isolated core complex in fractions 17–20 of the step gradient (lane 3) were probed by immunodetection using antibodies against outer and inner envelope proteins as indicated. (D) The purified core complex (fraction 17–20) was subjected to an S500-sephacryl size exclusion chromatography. The fractions indicated on top were subjected to SDS-PAGE followed by immunodecoration using Toc159, Toc75, or Toc34 antisera. The retention time of standard proteins is indicated by their molecular mass (numbers on the bottom). (E) The purified core complex was subjected to a superose 6 column, and peak fractions were used for EM (inset, left). The micrograph shows negatively stained particles (oval) at a magnification of 60,000 using the deep stain technique. The arrow points to tobacco mosaic virus, which was added for calibration purpose and as a standard to visualize the quality of the stain. The inset shows the profile of the size exclusion chromatography (triangles show the positions of thyroglobin and ferritin, respectively; the fraction at 0.9 ml represented the void volume and the fraction at 1.8 ml the salt peak). Bar, 100 nm.

by (a) formation of contact sites between outer and inner envelope (Nielsen et al., 1997), (b) interaction with HSP100 and HSP60 (Kessler and Blobel, 1996; Nielsen et al., 1997), and (c) assembly of at least a part of the translocation pore (Heins et al., 2002). For the other proteins it could only be demonstrated that they can be copurified with Tic110 or chemically cross-linked to a preprotein containing a transit peptide (Caliebe et al., 1997; Kouranov et al., 1998; Stahl et al., 1999; Küchler et al., 2002), but not much is known about their function during translocation. Here we describe

the isolation of the outer envelope translocon (Toc) of ~500 kD containing the 86-kD fragment of Toc159, Toc75, and Toc34 and analyzed its function, lipid content, and structure by transmission EM.

## Results

### The Toc forms a stable core complex of ~500 kD

Outer envelope membrane vesicles (equivalent to  $10 \pm 2$  mg of protein) were purified from intact chloroplast from

pea mesophyll cells by a modified procedure (Seedorf et al., 1995) outlined in the supplemental Materials and methods (available at <http://www.jcb.org/cgi/content/full/jcb.200210060/DC1>). Unfortunately, the time-consuming (8 h) procedure resulted in complete degradation of the intact Toc159 to a more stable fragment of 86 kD (Bölter et al., 1998; Bauer et al., 2000; Chen et al., 2000). However, none of the other Toc components tested were degraded during the purification process. The outer envelope vesicles still contained both small and large subunit of the ribulose 1,5-biphosphate carboxylase-oxygenase (RUBISCO) complex (Fig. 1 A, the large subunit is indicated by LSU). Furthermore, small amounts of inner envelope proteins were detected (Fig. 1 C, Tic40 and Tic110). These polypeptides have been described to occur as cross-contamination in all envelope preparation methods described (Stahl et al., 1999).

After solubilization of outer envelope membranes with 1.5% *n*-decyl- $\beta$ -maltoside, the mixture was fractionated by linear sucrose density gradient centrifugation (Fig. 1 A). This gradient removed the main contaminants (Fig. 1 A). The fractions containing the Toc components Toc159, Toc75, and Toc34 also contained the pore forming proteins OEP21 (Bölter et al., 1999) and OEP16 (Pohlmeier et al., 1997) (Fig. 1 C, lane 1). Therefore, these fractions (Fig. 1 A, indicated by a gray bar on top of the gel) were pooled, treated with a phospholipase, and fractionated again by centrifugation on a sucrose step gradient (Fig. 1 B). All major contaminants were removed in this way. In addition, Toc64 was absent from the purified complex (as explained in Discussion). We refer to the purified import complex consisting of Toc159, Toc75, and Toc34 as the Toc core complex.

The Toc core complex was further analyzed by size exclusion chromatography using several different column materials, e.g., S500-sephacryl or superose 6 (Fig. 1 E, inset). Fractions were tested for the presence of the Toc components by immunoblotting (Fig. 1 D) and silver staining (Fig. 1 E, inset). The Toc core complex eluted predominantly at  $\sim$ 500 kD (Fig. 1 E, inset) and contained only Toc159, Toc75, and Toc34 (Fig. 1 E, left, and D, lane 7). This fraction was further analyzed by transmission EM, which revealed homogeneous particles (Fig. 1 E). Due to extended time ( $\sim$ 1 h) for the gel filtration, we assume some of the Toc complex recovered from the sucrose density gradient (Fig. 1 B) disassembled or even aggregated during further purification (Fig. 1 D, lanes 3, 9, and 17, respectively). These complex populations were discarded and excluded from further analysis. Furthermore, we continued the sucrose centrifugation of the density gradient to equilibrium (78 h centrifugation versus 4 h in the purification process) in order to obtain a reliable estimate of the molecular mass of the core complex. The core complex of the outer envelope translocon migrated in the same fraction as RUBISCO, which has a size of 540 kD, indicating that the isolated complex has indeed roughly the same mass (unpublished data).

The stoichiometry of the Toc complex purified as described in Fig. 1 B was analyzed by comparing the amounts of Toc75, Toc34, and the 86-kD fragment of Toc159 present in the outer envelope or of overexpressed Toc75 (Sveshnikova et al., 2000a) and Toc34 (Sveshnikova et al., 2000b) by Coomassie brilliant blue staining and comparison

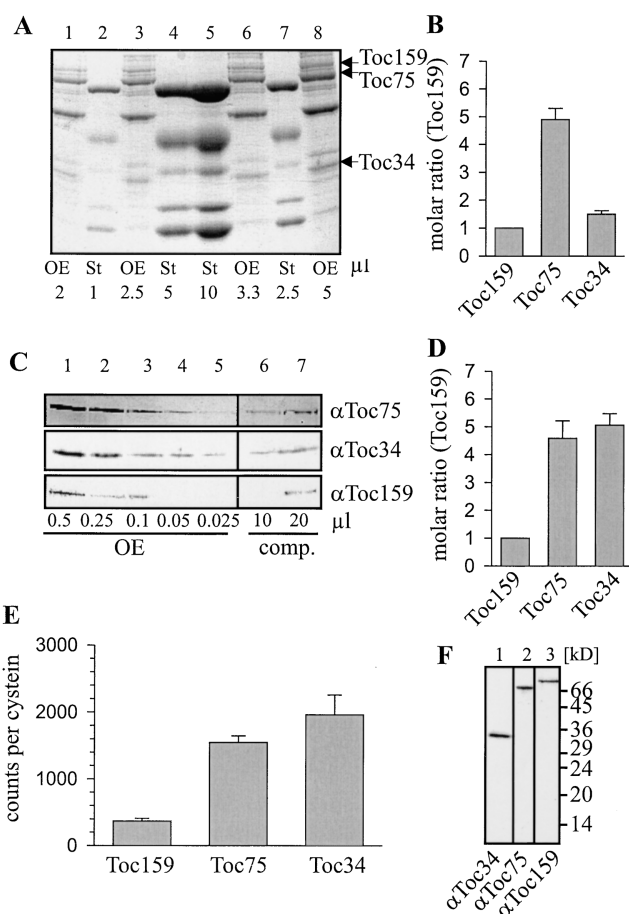


**Figure 2. Stoichiometry of the Toc components in the isolated core complex.** (A) Different amounts of calibration proteins (st.; lane 2, 4, 5, and 7) and outer envelope (OE; lane 1, 3, 6, and 8) were separated on SDS-PAGE followed by Coomassie brilliant blue staining. Toc34, Toc75, and the 86-kD fragment of Toc159 are indicated. (B) The molar quantity of the proteins was compared and normalized to the amount of Toc159 according to the staining in A. (C) Different amounts of outer envelope (lanes 1–5) and of the isolated Toc core complex (lanes 6 and 7) were separated on SDS-PAGE and immunodecorated using Toc159, Toc75, and Toc34 antibodies. (D) The molar amount of the proteins was compared and normalized to Toc159 (as in C). (E) The Toc core complex was treated with  $^3\text{H}$ -NEM. Incorporated radioactivity is counted and normalized to the number of cysteines in each protein. Histograms in B, D, and E show the average of at least three independent experiments. A representative figure is shown in A and C, respectively. (F) A Western blot analysis of the used purified Toc complex using antisera against Toc34 (lane 1), Toc75 (lane 2), and Toc159 (lane 3) is shown.

to molecular weight standards (Fig. 2 A and unpublished data). Intact Toc159 represents in general  $<5\%$  in the outer envelope preparations, and therefore the 86-kD fragment was analyzed. We observed a ratio of 1:5:1–2 molecules between Toc159, Toc75, and Toc34 in the outer envelope in situ, indicating that some free Toc75 exists in the envelope membrane besides assembled Toc complexes (Fig. 2 B). However, a similar analysis of the isolated core complex resulted in a different ratio of 1:4:4–6 molecules Toc159: Toc75: Toc34. In addition, outer envelope (Fig. 2 C) or purified Toc34 and Toc75 were immunodecorated with antibodies raised against Toc34, Toc75, and Toc159 (unpub-

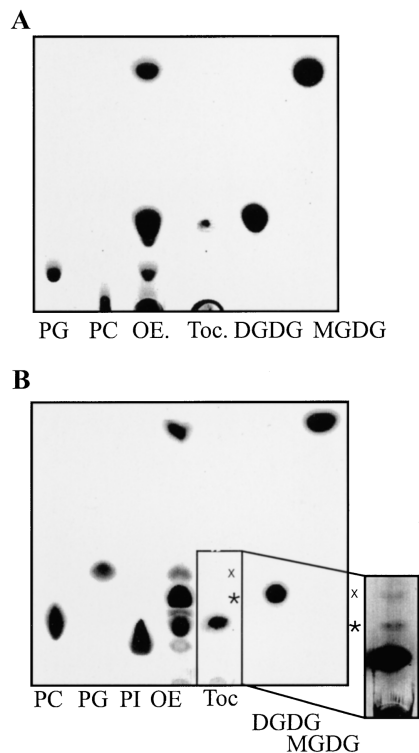


**Figure 3. Lipid analysis of the Toc core complex.** Lipids of the outer envelope (OE) and the core complex (Toc) after (A) and before (B) lipase treatment were separated using a mixture of acetone/benzene/water (A) or chloroform/methanol/water/acetic acid/acetone as solvent system (B). PC, PG, phosphatidylinositol (PI), MGDG, and DGDG are shown as standards. The inset shows the same result as in B with less contrast. x shows the position of PG and \* shows the position of DGDG.

lished data). By comparing their staining intensity, a ratio of 1:4–5:4–6 molecules was determined (Fig. 2 D). Since both methods are limited by the linearity of the stain intensity, we used a third approach. The cysteine residues of the proteins of the isolated core complex were labeled by radioactive (NEM) *N*-ethylmaleimide. After isolation of the proteins, the incorporated radioactivity was measured and normalized to the amount of cysteines present in each molecule (Fig. 2 E). The efficiency of labeling was controlled by a simultaneous treatment of overexpressed Toc34 and Toc75 (unpublished data), and the integrity of the proteins of the Toc complex was controlled by Western blot analysis (Fig. 2 F). This analysis revealed a molecular ratio of 1:4:4–5. A composition of 1:4:4 adds up to a calculated molecular mass of ~522 kD, consistent with the formerly observed apparent molecular mass of ~500 kD. From these results we propose that one copy of Toc159, four copies of Toc75, and four to five copies of Toc34 form the core complex.

#### Monogalactosyldiacylglyceride does not interact with the core complex of the outer envelope translocon

The chloroplast outer envelope shows a unique lipid composition of monogalactosyldiacylglyceride (MGDG; 17 mol%) digalactosyldiacylglyceride (DGDG; 29 mol%), phosphatidylcholine (PC; 32 mol%), phosphatidylglycerol (PG; 10 mol%), sulfoquinovosyl-diacylglyceride (6 mol%), and

phosphatidylinositol (6 mol%) (Schleiff and Klösgen, 2001). Several transit sequences reveal a high affinity for membranes containing the nonbilayer forming galactolipid MGDG. It was suggested that MGDG might be required for binding of the transit sequence as initial step before its recognition by the protein components of the Toc complex (Bruce, 2001). Therefore, we analyzed the lipid content of the isolated complex, anticipating that MGDG might be found as a part of the translocon. However, analysis of the purified core complex revealed only DGDG (the bilayer forming galactolipid of the outer envelope) but not MGDG (Fig. 3 A, lane Toc). Since the complex was treated with phospholipase during the purification procedure, we also investigated the lipid content of the complex purified without lipase treatment (Fig. 3 B). Now the major lipid detected was PC; however, low amounts of DGDG and PG were also present (Fig. 3 B, inset). As before, we did not detect MGDG. We conclude that the complex contains a specific subset of polar lipids, namely DGDG, PC, and some PG, which might be important as annular lipid in translocon function.

#### The Toc core complex binds preproteins in a GTP-dependent manner

To demonstrate that the isolated core complex was biologically active, the interaction of preproteins with the Toc core complex was analyzed. *In vitro*–translated radioactively labeled precursor of the small subunit of RUBISCO (preSSU) was incubated with the Toc core complex in the presence of EDTA or in the presence of GTP. The mixture was subjected to a sucrose step gradient to separate the complex bound form from free precursor. In the absence of Toc complex (Fig. 4 A, top) or in the presence of EDTA (Fig. 4 A, middle), preSSU did not enter the gradient. In the presence of GTP, preSSU was recovered in the same fraction as the Toc components (Fig. 4 A, bottom, and B), indicating a specific interaction. Further, preSSU heterologously expressed with a COOH-terminal hexahistidine tag was coupled to a nickel NTA column and incubated with the Toc core complex. In the presence of EDTA, no specific interaction with preSSU was observed (Fig. 4 C, lane 3). The proteins of the core complex were only found in the flow through (Fig. 4 C, lane 1). PreSSU could only be eluted by imidazol (Fig. 4 C, lane 3) but not by EDTA (Fig. 4 C, lanes 1 and 2). In the presence of GTP and  $MgCl_2$ , the Toc complex bound to the affinity matrix and eluted together with preSSU after addition of imidazol (Fig. 4 C, lane 6), indicating a specific interaction with the precursor protein. This interaction is specific for GTP, since ATP did not support or stimulate binding to the Toc complex (Fig. 4 D, lanes 2 and 4). In contrast, when GDP was added together with GTP the interaction was reduced (Fig. 4 D, lane 5), which is in line with the observation that GDP alone could not support the interaction (Fig. 4 D, lanes 4 and 6). To test if the Toc complex specifically interacts with the transit sequence, the precursor form and the mature form of SSU and a synthetic transit sequence peptide were covalently coupled to an activated matrix and incubated with purified Toc complex in the absence and presence of guanylyl-imidodiphosphate (GMP-PNP), the nonhydrolyzable homologue of GTP. We observed a reduction of the background in the binding ex-

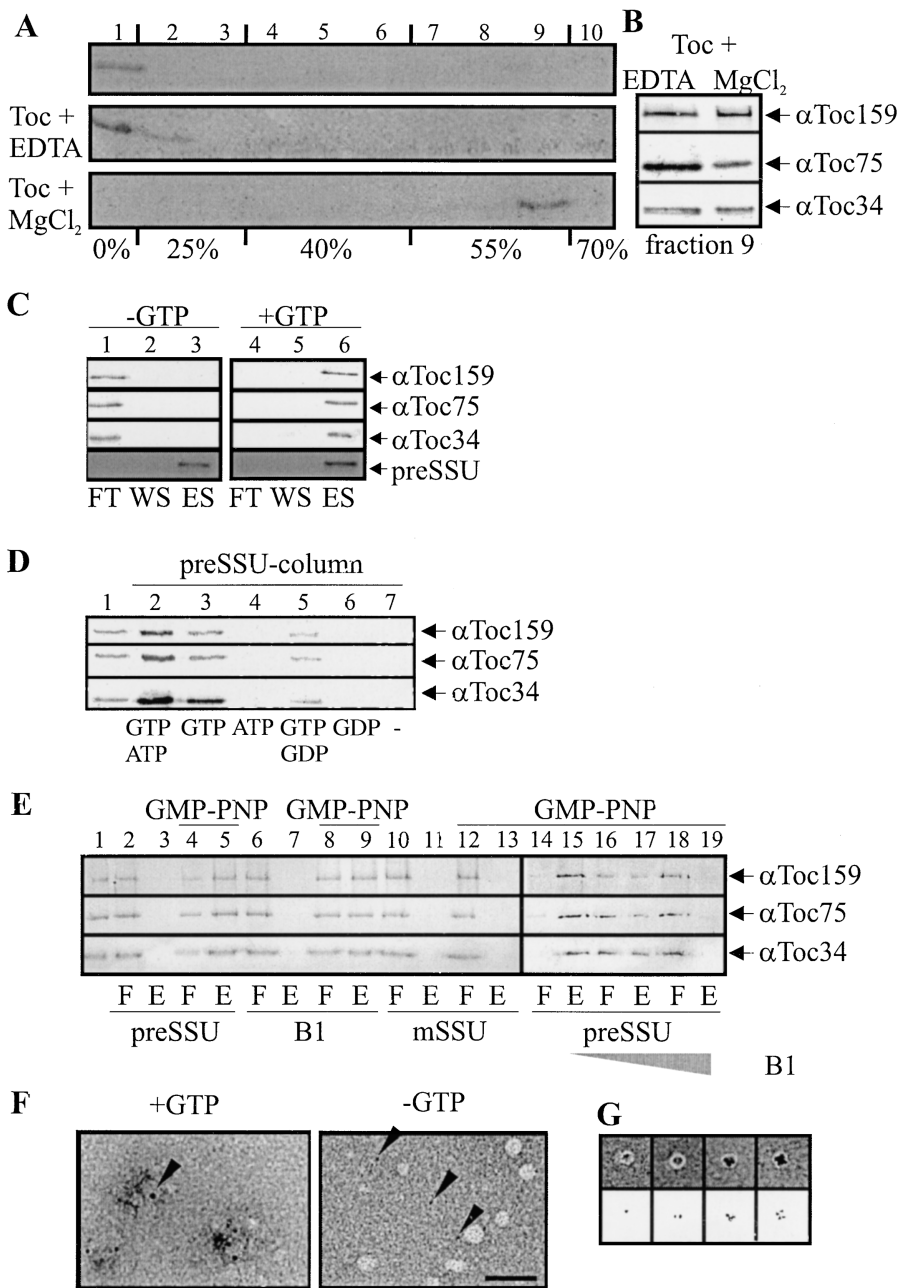


**Figure 4. Functional analysis of the isolated complex.** (A) Radioactive-labeled preSSU was subjected on top of a step gradient before (top) and after incubation with the isolated Toc complex in the presence of 0.1 mM EDTA (middle) or 1.0 mM  $MgCl_2$  (bottom) and 0.5 mM GTP and centrifuged. Fraction numbers are indicated on top, and the percentage of the sucrose is given below the figure panel. (B) Fraction 9 of the gradient containing EDTA (left) or  $MgCl_2$  (right) was probed using antisera against Toc159, Toc75, and Toc34 as indicated. (C) Heterologously expressed preSSU-His<sub>6</sub> was coupled to an affinity matrix and incubated with the isolated Toc complex in the absence (lane 1–3) or presence of 0.5 mM GTP and 1 mM  $MgCl_2$  (lanes 4–6). Proteins in flow through (FT), wash step (WS), and elution with 0.25 M imidazol (ES) were precipitated, resolved in Laemmli sample buffer, separated by SDS-PAGE, and immunoblotted using  $\alpha$ Toc159,  $\alpha$ Toc75, and  $\alpha$ Toc34 antibodies or silver stained to visualize preSSU. (D) The experiment was performed as in C, but only eluted fractions are shown. Lane 1 shows the loaded complex (20%) and lanes 2 to 7 show the eluted fractions after binding in the presence of 0.25 mM GTP/0.25 mM ATP (lane 2), 0.25 mM GTP (lane 3), 0.25 mM ATP (lane 4), 0.25 mM GTP/0.25 mM GDP (lane 5), 0.25 mM GDP (lane 6), and without nucleotides (lane 7). (E) Purified Toc complex was added to preSSU (lanes 2–5 and 14–19), mSSU (lanes 10–13), or synthetic B1 peptide (lanes 6–9) coupled to Toyopearl matrix in the absence (lanes 2, 3, 6, 7, 10, and 11) or presence of GMP-PNP (lanes 4, 5, 8, 9, and 12–19) after preincubation with 5  $\mu$ M (lanes 16 and 17) and 50  $\mu$ M (lanes 18 and 19) B1 peptide. 50% of the used Toc fraction (lane 1), the flow through (F, even lanes), and the bound fractions (B, uneven lanes) were separated on SDS-PAGE followed by immunodecoration using antisera against Toc159, Toc75, and

Toc34. (F) Transmission EM of Toc complex treated with the peptide covalently linked to nanogold particles in the absence (right) or presence of 0.5 mM GTP and 1 mM  $MgCl_2$  (left). In the presence of 0.5 mM GTP, 90% of the observed gold particles (arrowheads) were shown to be associated to Toc complex clusters, whereas under nonbinding conditions the gold appeared to be randomly distributed over the carbon surface. (G) Representative complexes with one to four (from left to right) gold particles are shown (top), increasing the contrast to show the gold particles (bottom).

periments in the presence of GMP-PNP compared with experiments in the presence of GTP, whereas the overall binding behavior was not altered (unpublished data). Therefore, GMP-PNP was used. The Toc complex associated with the matrix-bound synthetic transit peptide (B1) and the precursor form of SSU in the presence of GMP-PNP (Fig. 4 E, lanes 5 and 9) but not in the absence of nucleotide (Fig. 4 E, lanes 3 and 7). In contrast, matrix-bound mSSU could not interact with the purified Toc complex even in the presence of GMP-PNP. The Toc complex was only detected in the flow through (Fig. 4 E, lanes 10 and 12), and no Toc sub-

units were detected in the eluat (Fig. 4 E, lanes 11 and 13). This indicates a specific interaction of the Toc complex with the transit sequence. Our observation is supported by the finding that the synthetic transit peptide (B1) can compete for the interaction of the Toc complex with preSSU in the presence of GMP-PNP (Fig. 4 E, lanes 14–19). In the absence of competitor, almost all of the Toc complex (>80%) was bound to the preSSU affinity matrix (Fig. 4 E, lanes 5 and 15). Addition of 5  $\mu$ M of the peptide reduced the interaction already to ~50% (Fig. 4 E, lane 17), and in the presence of 50  $\mu$ M transit peptide the Toc complex did no

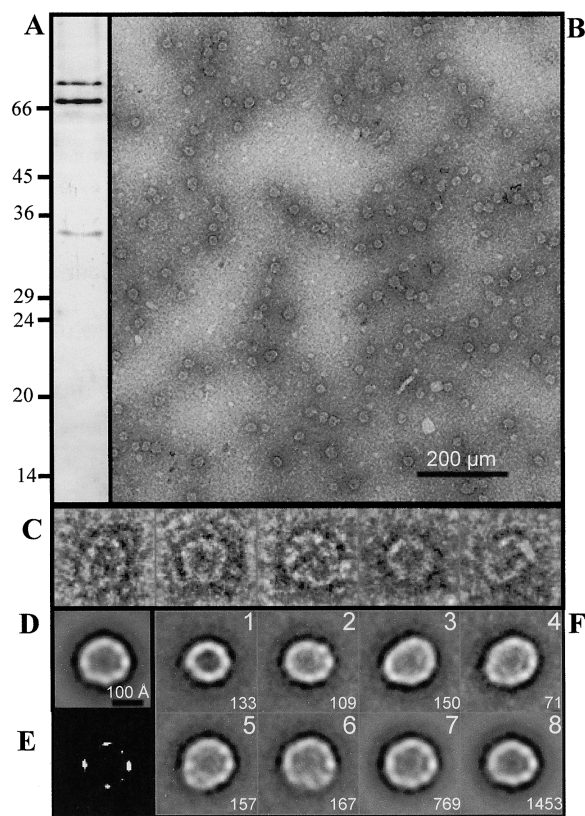


**Figure 5. Two-dimensional single particle analysis.** (A) A silver-stained gel of the sample used is shown. (B) An electron micrograph of the sample recorded as described using the two-layer carbon technique is shown. A gallery of selected Toc complex particles (C) and the average of 3,207 aligned images is shown (D). (E) At very high contrast, only the densest regions of the image are visible. (F) Particles were classified into eight classes. The numbers in the lower right corner represent the number of images comprising each class. See also Fig. S1 available at <http://www.jcb.org/cgi/content/full/jcb.200210060/DC1>.

longer associate with the affinity matrix (Fig. 4 E, lane 19). The association of the complex with the transit peptide was also investigated by transmission EM (Fig. 4, F and G). First the transit peptide was coupled to 5 nm gold particles. When the complex was incubated with the gold-labeled peptide in the presence of GTP, the gold was only found associated with complexes (Fig. 4 F, +GTP). The low contrast of the micrograph results probably from the high density of the gold particles within the Toc complex or a variation in the negative staining. Interestingly, we could identify up to four gold particles within one complex (Fig. 4 G). In contrast, in the absence of GTP no specific association of the gold-labeled peptide with Toc particles was observed (Fig. 4 F, -GTP), again suggesting that the association of transit sequences is strongly GTP dependent.

### Structural analysis of the isolated complex

To gain insight into the structural composition of the Toc core complex, we imaged the purified assembly (Fig. 5 A) by transmission EM of negatively stained specimens sandwiched between two layers of carbon (Fig. 5 B). A gallery of particles is shown in Fig. 5 C. The average of 3,207 aligned

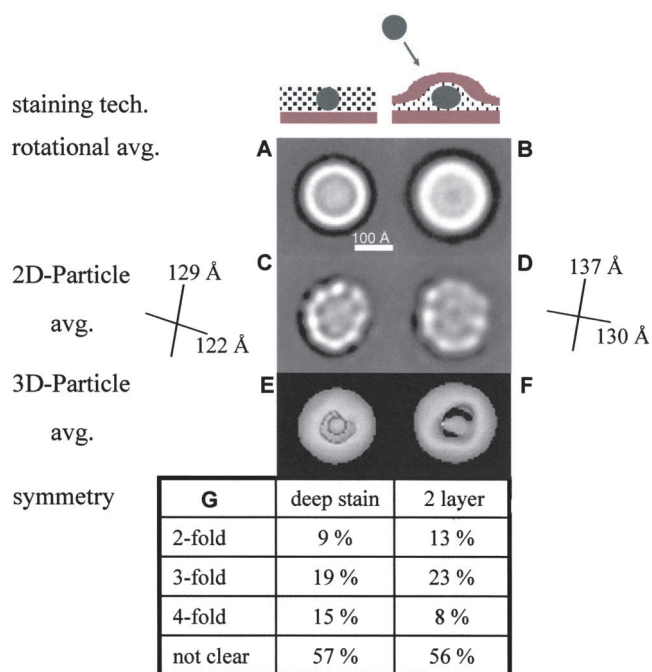


**Figure 6. Symmetry of the particles by comparing the two-layer carbon and deep stain technique.** Size and shape of the Toc complex particles in deep stain (A, C, and E) and two-layer carbon stain (B, D, and F) were determined at a calibrated magnification of 58,300 $\times$ . A and B show the average of centered particle images before rotational alignment (4,028 images in A and 2,058 images in B). C and D are the averages of the rotationally and translationally aligned two-dimensional images, respectively. E and F show the average of the three-dimensional reconstructions. (G) Results of rotational symmetry analysis of the two-dimensional particles are listed.

particles shows a toroid structure with a solid rim and less dense stain-excluding material in the center (Fig. 5, D and E). A classification procedure divided the particles into eight classes (Fig. 5 F). Classes 2 to 8 differed only slightly in terms of shape or apparent internal structure. Classes 7 (25% of all particles) and 8 (50% of all particles) represent the most predominant structure of the isolated Toc core complex. A small number of the particles (4.5%) fell into class 1, which looked significantly different from the other classes. The particles are smaller and show higher contrast. Therefore, we believe that this smaller particle either represents a minor form of the Toc complex in a different conformation or a minor contaminant. We could not determine if this particle is formed during the purification procedure or during preparation of the probes for EM. It might represent a channel with dissociated receptor proteins or might be a result of further proteolysis of Toc159 to the 52-kD fragment.

The EM of the complex was then repeated using a controlled deep layer of stain, which reduces the distortion of the particles on the carbon film (Fig. 6). In this way we achieved a better presentation of the complex. The rotational average representing the average of all particles after translational but before rotational alignment gives an impression of the distribution of density within the complex. With both staining techniques, the rotational average yields very similar distributions of density within the particle, namely a strong outer ring, and a less dense and less clearly

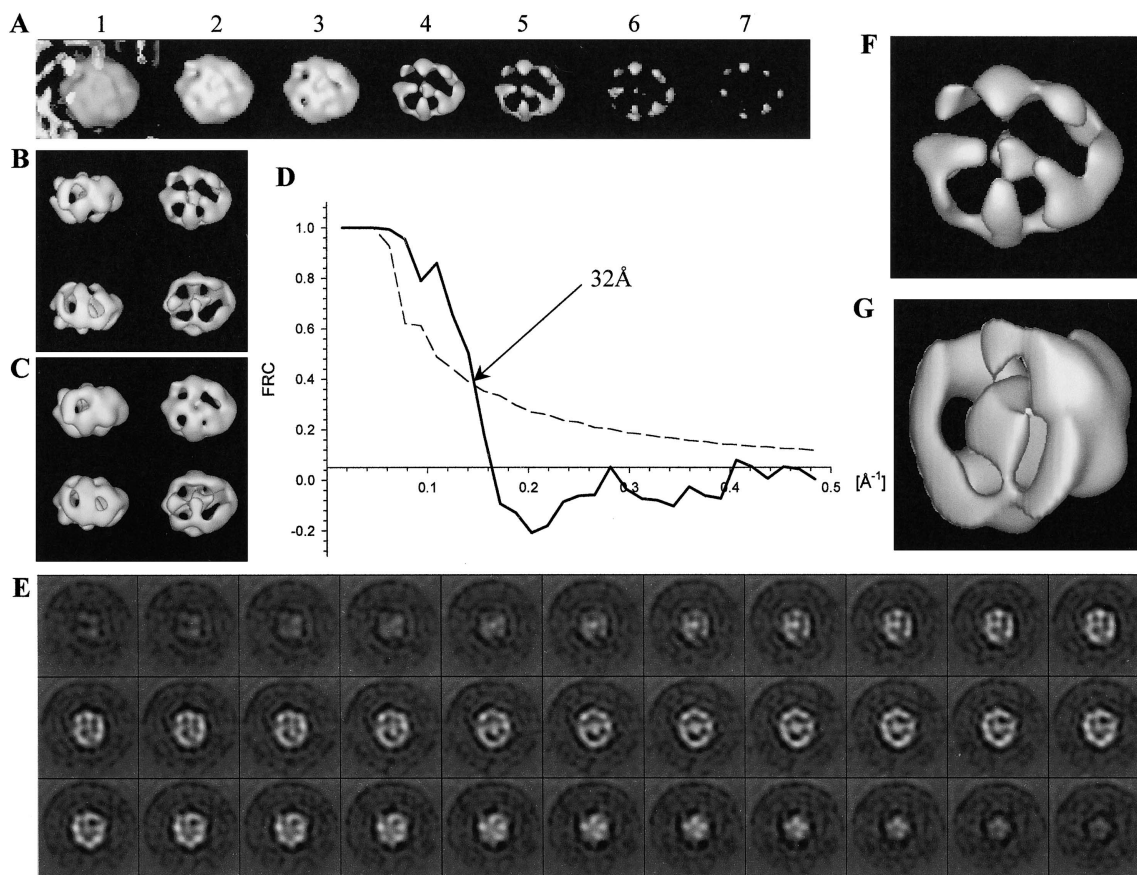


**Figure 7. Three-dimensional volume of the core complex.** The three-dimensional volume of a class comprising 679 particles shown as rendered volume surface (A–C, F, and G) as a series of slices perpendicular to the z axis. (A) A threshold series of the top view is given starting at low threshold (1). (B) The side view (top left) and top view (top right) of the volume at threshold similar to 4 in A is shown. The bottom part shows the volume rotated by 180° along the z axis. C shows the same views at a lower threshold. (D) The Fourier ring correlation and noise correlation reference curves indicate a resolution of 32 Å. (E) A series of z slices spaced by 3.5 Å. (F) The top view at the same threshold as in 4 (A) is shown enlarged. (G) The left half of the volume is removed to reveal the interior structure.

structured center (Fig. 6, A and B). The average of the two-layer carbon technique suggests also a cavity in the very center, but this was not confirmed by deep stain. As expected, the translationally and rotationally aligned particles (Fig. 6, C and D) show more detail. The region between the outer ring and the central density suggests several darkly stained regions, which might represent translocation pores. Therefore, we conclude that a dense outer protein ring and a less dense central protein structure form the core complex of the outer envelope translocon of chloroplasts. The dimensions of the complex are  $\sim 6\%$  smaller in deep stain. However, the diameters of the x and y direction differ by 0.7 nm independent of the staining technique. The particles appear to be nonsymmetrical, since no significant twofold, threefold, or higher symmetry was detected (Fig. 6 G).

Random conical tilt reconstruction was performed in order to determine the low resolution three-dimensional structure of the complex. The average three-dimensional volumes calculated from all analyzed particles (Fig. 6, E and F) indicate a dense protein ring and a more complex central structure consistent with the two-dimensional analysis of the complex. Three-dimensional analysis with a completely independent dataset comprising 4,028 particles in deep stain was then performed. Again, classification (Fig. S1 avail-

able at <http://www.jcb.org/cgi/content/full/jcb.200210060/DC1>) revealed that 5% of all particles represent the small and contrast-rich minor fraction. All other classes contained particles with similar features as described above. The class including the highest number of particles (679) was chosen for three-dimensional reconstruction (Fig. 7). The resolution of 32 Å based on the Fourier ring correlation criterion (Van Heel, 1987) (Fig. 7 D) reflects the number of particles used. The volumes have dimensions of 100–125 Å in height and a diameter of 120–140 Å (Fig. 7, B and C). The Toc complex seems to contain four independent pores. This is evident when density threshold of the surface representation is increased (Fig. 7, A–C). In line with the projection maps (Fig. 5), the complex consists of a dense outer ring-like structure, a central density, and four bridges to the central region. The presence of a connection between the bridges and the central “finger” domain depends on the threshold chosen (Fig. 7, A–C). On the opposite surface only one bridge-like structure points to this central finger domain. Slices perpendicular to the z axis (Fig. 7 E) revealed that the pores seem to be open on one side but closed on the other. Furthermore, it seems that the channels are twisted and possibly connected in the center of the particle. This can also be seen when the particle is divided in the middle (Fig. 7 G,

shown is the right half of the particle). We conclude that the Toc complex forms four independent pores, which might be connected in the interior of the complex. This is in line with the complex stoichiometry, suggesting four Toc75 channels per complex.

## Discussion

A detailed analysis of the molecular mechanism of protein translocation requires the quantitative isolation and structural analysis of the translocation complexes. Several methods were used in the past to isolate, for example, the mitochondrial translocon (Kunkele et al., 1998; Model et al., 2001), the Sec machinery of bacteria (Manting et al., 2000; Collinson et al., 2001), or the TAT complex of *Escherichia coli* (Bolhuis et al., 2001; Sargent et al., 2001). Most of these techniques were based on gene manipulation and subsequent purification by affinity chromatography.

The purified core complex presented here contains three of the four known subunits of the Toc complex, namely the 86-kD fragment of Toc159, Toc75, and Toc34 (Fig. 1). Toc64 was not detected, suggesting that this component is transiently associated with the core complex. In addition, the comparison of the stoichiometry of the three core components present in the outer envelope and in the isolated complex (Fig. 2) also suggests that only 25% of the total amount of Toc75 may be present in the isolated core complex. The molecular ratio of Toc75 and Toc34 in the outer envelope in situ is close to 4:1, whereas the ratio in the complex is nearly 1:1. This may have several reasons. Recent observations suggest that the Toc complex is a dynamic ensemble (Hiltbrunner et al., 2001a). Therefore, the association of Toc34 might be transient as proposed for Toc64, and this association may be regulated by phosphorylation (Sveshnikova et al., 2000b) or GTP hydrolysis (Jelic et al., 2002; Sun et al., 2002). On the other hand, Toc75 might be involved in the formation of different isoforms of the Toc complex (Jarvis et al., 1998; Bauer et al., 2000). This might suggest either that an independent Toc75–Toc64 complex exists, that Toc75 itself is involved in protein translocation of OEPs, or that an inactivated pool of Toc75 exists for assembly of additional translocation complexes under different requirements for protein import into chloroplasts.

The isolated complex revealed a stoichiometry of 1:4:4–5 molecules of Toc159, Toc75, and Toc34 (Fig. 2). This is consistent with an apparent molecular mass of ~500 kD (Fig. 1) and the results of EM, which also suggests a non-symmetrical stoichiometry (Fig. 6) and a particle of this size. Earlier cross-link analysis of the translocation complex revealed a molecular mass of ~700 kD (Akita et al., 1997). However, this cross-linked complex contained also the Tic component Tic110, the precursor protein preSSU, and HSP100. The Toc complex described here (~500 kD) and the identified Tic complex (280 kD) containing HSP100 (Caliebe et al., 1997) add up to roughly this mass.

The transport of preproteins through the cytosol can involve a heterooligomeric precursor complex (May and Soll, 2000). It remains to be investigated if the transit sequence is directly transferred to the cytosolic domains of the receptor proteins (Hiltbrunner et al., 2001a) or if an intermediate lipid association is essential (Bruce, 2001). Our results indi-

cate that the Toc core complex does not contain MGDG (Fig. 3), a nonbilayer lipid proposed to be the major component for the interaction with transit sequences (Bruce, 2001), suggesting that such an intermediate step is unlikely for the in vivo process. However, PC is the major lipid associated with the complex before phospholipase treatment. This is not surprising, since PC is the most abundant lipid of the outer envelope. It was demonstrated that treatment of chloroplasts with PLC abolished preprotein translocation but not recognition (Kerber and Soll, 1992). How PC interferes with preprotein translocation remains to be demonstrated, since PC is not required for complex stability. Interestingly, the complex is also associated with PG and DGDG. PG is only present in the inner leaflet of the outer envelope (Dorne et al., 1985). It could be speculated that PG might function as an additional component in the translocation process by attracting the positively charged transit sequences toward the intermembrane space.

The structure of the core complex of the Toc translocon has a toroid shape as revealed by projection maps obtained by electron image analysis. The particle clearly shows a dense ring around its perimeter and a less dense structure in the center. The average three-dimensional map revealed a central “finger” domain. This finger domain divides the central cavity into four apparent pores. The particle itself has a diameter of 13 nm and a height of 10–12 nm.

The estimated heights of the complex (10–12 nm) is higher than the estimated thickness of the outer envelope membrane. This could be due to two reasons: first, Toc159 and Toc34 protrude with large domains into the cytosol, and second, the structural prediction for Toc75 indicates that the import channel comprises large loop regions (Sveshnikova et al., 2000b). The five domains seen in the threshold series (Fig. 7 A) and in the enlarged view (Fig. 7 F) possibly represent the soluble domains of Toc34 and Toc159, which would correlate well with the observed stoichiometry (Fig. 3). The interaction of four of these domains with the central finger domain might be formed by the cytosolic domains of the receptor subunits. Further, the simultaneous interaction of four peptides with the complex (Fig. 5 E) suggests the presence of four independently acting translocation pores within one complex. The interior structure of the particle suggests that the channels are twisted and might be connected in its center. At this resolution we cannot distinguish between a structure composed of four channels formed by the individual Toc75 or an outer ring formed by Toc75 and an interior structure composed of soluble domains interacting with the membrane-facing regions of the exterior. The electron microscopic pictures only give an estimate of the pore size at the channel entrance of ~20–40 Å (Fig. 7, B and C) but not of its most narrow diameter inside. However, the pore size estimated by electrophysiological studies (~2 nm) (Hinnah et al., 2002) assemble well the observation presented here. However, if future structure analysis by electron cryomicroscopy confirms the presence of four pores in the Toc complex, it is tempting to speculate that each pore is formed by Toc75 and Toc34 and that the four pores assemble around one copy of Toc159, which might then form a part of the central finger-like domain.

## Materials and methods

### Materials and antibodies

*N*-[ethyl-1-<sup>14</sup>C]-maleimide was purchased from NEN Life Science Products. The S400-sephacryl, S500-sephacryl, and G25-sephadex material, the superose 6 column for size exclusion chromatography, and Percoll was supplied by Amersham Biosciences. The peptide B1-C (MVPFTGLK-SAASFPVSP<sup>R</sup>RKQNLDTIS-C) was synthesized at the Department of Peptide and Protein Chemistry at the Charité. *n*-decyl- $\beta$ -maltoside was purchased from Glycon GmbH. Protein concentration was determined using the Bio-Rad Laboratories' protein assay. All other chemical used were purchased from Roth or Sigma-Aldrich. The production of the used antibodies was described earlier for Tic110 (Waegemann et al., 1992), Toc159 (Waegemann and Soll, 1991), Toc75 (Hinnah et al., 1997), Toc64 (Sohrt and Soll, 2000), Tic40 (Stahl et al., 1999), Toc34 (Seedorf et al., 1995), OEP24 (Pohlmeyer et al., 1998), OEP21 (Bölter et al., 1999), and OEP16 (Pohlmeyer et al., 1997). OEP37 antibodies were raised in rabbits against a heterologously expressed His tag containing protein (Schleiff et al., 2003).

### Toc core complex preparation

0.5 mg outer envelope purified as described in the supplemental Materials and methods (available at <http://www.jcb.org/cgi/content/full/jcb.200210060/DC1>) was pelleted at 202,000 *g* for 10 min at 4°C and resuspended in 300  $\mu$ l of 25 mM Hepes/KOH, 100 mM NaI, 1 mM  $\beta$ -mercaptoethanol, and 1.5% *n*-decyl- $\beta$ -maltoside, pH 7.0, except otherwise noted. After 10 min, the solubilized outer envelope was layered on top of a 25–70% (wt/vol) sucrose gradient (in 25 mM Hepes, 100 mM NaI, 1 mM  $\beta$ -mercaptoethanol, 1 mM EDTA, and 0.075% *n*-decyl- $\beta$ -maltoside, pH 7.0) and centrifuged for 4 h at 320,000 *g* at 4°C using a swinging bucket rotor. The fractions containing the Toc complex of at least six gradients were pooled, diluted four times using 25 mM Hepes, 100 mM NaI, 1 mM  $\beta$ -mercaptoethanol, pH 7.0, and incubated with lipase VII (Sigma-Aldrich) for 30 min at 4°C before layering on top of a step gradient. The step gradient was composed of 25%:45%:55%:70% (wt/vol) sucrose in 25 mM Hepes, 100 mM NaI, 1 mM  $\beta$ -mercaptoethanol, 1 mM EDTA, and 0.075% *n*-decyl- $\beta$ -maltoside, pH 7.0. After centrifugation for 16 h at 285,000 *g* at 4°C, complex fractions were harvested and pooled. For lipid extraction, the pooled fractions were used directly. For other experiments, the complex fractions were diluted with the same volume of 25 mM Hepes, 100 mM NaI, 1 mM  $\beta$ -mercaptoethanol, 1 mM EDTA, and 0.075% *n*-decyl- $\beta$ -maltoside, pH 7.0, and concentrated by centrifugation for 16 h at 285,000 *g* at 4°C on top of a 70% (wt/vol) sucrose layer. The complex was frozen in liquid nitrogen and stored at –20°C.

### Determination of the stoichiometry of the Toc core complex

Determination of the numbers of Toc159, Toc75, and Toc34 molecules present in the outer envelope was performed as described (Tyedmers et al., 2000). Different amounts of outer envelope membranes (5 mg/ml) or overexpressed Toc75 and Toc34 (0.5 mg/ml each) were subjected to SDS-PAGE, and the intensity of the Coomassie brilliant blue R250-stained bands within the linear range was compared with the following proteins:  $\alpha$ -lactalbumine (14.2 kD, 1 mg/ml), trypsin inhibitor (20.0 kD, 1 mg/ml), trypsinogen (24.0 kD, 1.25 mg/ml), carbonic anhydrase (29.0 kD, 0.25 mg/ml), glyceraldehyde-3-phosphate dehydrogenase (36.0 kD, 0.25 mg/ml), egg albumin (45.0 kD, 1.25 mg/ml), and BSA (66.0 kD, 1.25 mg/ml). Different amounts of either overexpressed Toc75 or Toc34 (0.5 mg/ml), outer envelopes (5 mg/ml), or isolated core complex were subjected to SDS-PAGE analysis followed by immunodecoration with Toc159, Toc75, or Toc34 antibodies. The density was quantified as described (Tyedmers et al., 2000). For NEM labeling, 0.1 ml core complex was denatured by incubation in 6 M guanidinium-HCl, pH 8.0, and 10 mM dithiothreitol for 24 h at 4°C. Dithiothreitol was removed by G25 Sephadex spin chromatography, and 5 mM NEM containing 0.37 MBq *N*-[ethyl-1-<sup>14</sup>C]-maleimide was added. After incubation for 15 min at 4°C, the complex was precipitated and resuspended in a buffer without NEM. The proteins were separated on a 10% SDS-PAGE, and gel slices containing protein were dissolved in perchloric acid and hydrogen peroxide and mixed with 10 ml of Rotiszint (ROTH). Radioactivity was quantified by scintillation counting.

### Lipid extraction

0.5 ml core complex solution or 300  $\mu$ g outer envelope was mixed with 2 ml of chloroform. 1 ml of methanol was added followed by vigorous mixing. After incubation on ice for 5 min, 6 ml chloroform/water (1:1 vol/vol) was added, and the mixture was centrifuged for 15 min at 3,000 *g* at 4°C. The chloroform phase was separated and dried under nitrogen. The lipid film of the complex fraction was dissolved in 20  $\mu$ l chloroform and the

lipid film of the outer envelope in 200  $\mu$ l chloroform. 10  $\mu$ l of each fraction was spotted on 10  $\times$  10 silica gel 60 plates (Merck) along with 2  $\mu$ g of standard plant lipids (Nutfield Nurseries). The lipids were dissolved by the following systems: acetone/benzol/water 45:15:4 (vol/vol/vol), chloroform/methanol/water 65:25:4 (vol/vol/vol), and chloroform/acetone/methanol/acetic acid/water 10:4:2:2:1 (vol/vol/vol/vol). The lipids were stained using 0.54 M H<sub>2</sub>SO<sub>4</sub>, 5.5 mM KMnO<sub>4</sub>, and FeSO<sub>4</sub>  $\times$  7H<sub>2</sub>O and visualized by heating for 10 min at 110°C.

### Binding analysis

In vitro transcription and translation was described elsewhere (Schleiff et al., 2001). PreSSU-His was overexpressed and purified as described previously (Sveshnikova et al., 2000b). Purified preSSU was dialysed into 25 mM Hepes, pH 7.0, and 100 mM NaI and incubated with 0.1 ml nickel matrix (QIAGEN) for 30 min at 20°C. After washing the matrix with 10 column vol of 25 mM Hepes, pH 7.0, and 100 mM NaI, Toc complex was passed over the matrix in the absence or presence of GTP. The column was washed again with 10 column vol of 25 mM Hepes, pH 7.0, and 100 mM NaI and preSSU eluted using 0.5 ml 250 mM imidazol, 25 mM Hepes, pH 7.0, and 100 mM NaI. All fractions were precipitated and subjected to SDS-PAGE analysis and immunoblotting.

PreSSU, mSSU, and synthetic B1 peptide (Schleiff et al., 2002a) were coupled to Toyopearl (TosoHaas Biosep) by the method described in Schleiff et al. (2002b). The purified Toc complex (1 ml containing 10  $\mu$ g protein) was incubated for 5 min in 20 mM Hepes, pH 7.6, 100 mM NaCl, 0.5 mM MgCl<sub>2</sub>, and 0.15% decylmaltoside with 10  $\mu$ l of the prepared affinity matrix in the absence or presence of 1 mM GMP-PNP. The affinity matrix was washed two times with 1 ml of the same buffer in the absence or presence of GMP-PNP. The remaining sample was eluted by addition of SDS sample buffer. For competition, indicated amounts of the synthetic B1 peptide were incubated with the Toc complex for 2 min in the presence of 1 mM GMP-PNP before addition of the affinity matrix. All fractions were precipitated and subjected to SDS-PAGE analysis and immunoblotting.

### Gold labeling of the transit sequence peptide B1-C

A quantity of 1.6 mM of the peptide B1 (Schleiff et al., 2002a) containing a COOH-terminal cysteine was incubated for 60 min at 25°C with 10 mM dithiothreitol in 0.1 M sodium phosphate, 5 mM EDTA, pH 6.0. Dithiothreitol was separated from the peptide by G25 Sephadex spin chromatography in 20 mM sodium phosphate, 150 mM NaCl, and 1 mM EDTA, pH 6.5, as running buffer. An amount of 6 nmol monomaleimido nanogold (5 nm; Nanoprobe) was dissolved in 20  $\mu$ l dimethyl-sulfoxide and diluted 10 times into water followed by addition of 500  $\mu$ l of the reduced peptide. After incubation for 18 h at 4°C, unlabeled peptides and monomaleimido nanogold was removed by passing the solution through thiol-activated sepharose (Sigma-Aldrich). Of the flow-through, 2  $\mu$ l was added to a solution containing pelleted Toc complex, 0.5 mM GTP, and 0.5 mM MgCl<sub>2</sub>. The reaction mixture was kept 2–5 min on ice and subsequently used for transmission EM. Instead of GTP and MgCl<sub>2</sub>, EDTA in a final concentration of 5 mM was used as a control in the labeling reaction.

### Size exclusion chromatography

Pelleted fractions of the sucrose density gradient containing the Toc complex were subjected to gel filtration on a S400-sephacryl, S500-sephacryl, or superose 6 column. Fractions were either collected by gravitation (S400 and S500) or using the SMART System (superose 6; Amersham Biosciences) at a flow rate of 40  $\mu$ l/min. The elution buffer contained 25 mM Hepes, pH 7.4, 150 mM NaI, and 0.15% *n*-decyl- $\beta$ -maltoside. The peak fractions were investigated by transmission EM. For size determination, Blue Dextran 2000 (2 MDa), thyroglobulin (669 kD), ferritin (440 kD), catalase (232 kD) (Amersham Biosciences), albumin (BSA, 68 kD), and chymotrypsin (25 kD) (Roche) were used as calibration proteins.

### EM

**Two-layer carbon films.** A 5- $\mu$ l drop of the undiluted sample was applied to a 400 mesh carbon-coated copper grid. After incubation for ~1 min, the grid was transferred to a 50- $\mu$ l drop of 2% ammonium molybdate, pH 6.5, and transferred to another drop of stain. A second layer of carbon was applied to the specimen, and excess staining solution was removed by placing the grid on a piece of filter paper (Whatman 4).

**Deep stain.** The technique is based on the method developed by Stoops et al. (1992). A drop of 5  $\mu$ l of the complex was applied to a carbon-coated copper grid. After incubation for 1 min, the grid was washed three times on drops of water, then once on a drop of 2% ammonium molybdate, pH 6.5. Finally, the grid was transferred to another drop of stain. After a 30-s incubation, the liquid was quickly removed, holding a filter paper (What-

man 4) for very short time to the edge of the grid. The grid was then dried in a steam of air at RT.

**Transmission EM.** Transmission EM was performed using either a Philips CM12 electron microscope at an accelerating voltage of 120 kV or a Philips CM120 electron microscope at an accelerating voltage of 100 kV. Micrographs were recorded under low dose conditions at underfocus between settings 1.2 and 1.8  $\mu\text{m}$  and magnifications of 45,000 or 60,000. For the random conical tilt reconstruction, a first image was recorded at 55–60° tilt, and a second image of the identical untilted specimen area was recorded. Tobacco mosaic virus was added for calibration.

**Image processing.** Micrographs were digitized with a 7- $\mu\text{m}$  pixel size on a Zeiss SCAI scanner. The image size was reduced by  $3 \times 3$  averaging resulting in 21- $\mu\text{m}$  pixels, which corresponds to 0.36 nm on the scale of the specimen. Particles were interactively selected and aligned with the SPIDER image processing software, essentially as described by Radermacher et al. (2001). The contrast transfer function was corrected (Radermacher et al., 2001). A first reference was created by reference-free alignment (Marco et al., 1996a,b). After three rounds of rotational and translational alignment, an overall average of the images was generated. Image classification was performed using a neuronal network algorithm (Marabini and Carazo, 1994) as implemented in XMIPP (Marabini et al., 1996) using a field of  $9 \times 9$  nodes. A certain number of nodes showing significant features of the particles was selected from the map and used as references in subsequent multireference alignment (Radermacher et al., 2001). Average images of each class were calculated. The resolution was determined by Fourier ring correlation (van Heel and Harauz, 1988) and comparison with  $5 \times$  noise. For three-dimensional reconstruction, the rotation angle of each projection was transferred to the corresponding projection of the tilted particle. Then, the rotational and tilt angle of each particle was known. Using the Radon transforms of the projections, the particle volumes were calculated. Refinement of the volumes was achieved by aligning the Radon transforms of the individual tilt images to the corresponding transforms of the initial volume (Radermacher, 1994).

**Analysis of rotational symmetry.** Analysis was performed as described by Pascual-Montano et al. (2001). A self-organizing map using the rotational power spectra of the images was generated. Then, nodes representing clearly defined symmetry (twofold, threefold, or fourfold) were selected and combined as symmetry classes (twofold, threefold, and fourfold). The number of the images assigned to each of the symmetry classes was compared with the total number of images and expressed as a percentage.

### Online supplemental material

Supplemental Materials and methods describe the outer envelope vesicle purification and the single particle analysis of the deep stain images. Fig. S1 shows the classification similar to the analysis of the double layer images in Fig. 5. Supplemental Materials and methods and Fig. S1 can be found at <http://www.jcb.org/cgi/content/full/jcb.200210060/DC1>.

This work was supported by grants from the Deutsche Forschungsgemeinschaft and the Human Frontier Science Program to J. Soll, W. Kühlbrandt, and E. Schleiff.

Submitted: 10 October 2002

Revised: 2 January 2003

Accepted: 2 January 2003

## References

- Akita, M., E. Nieslen, and K. Keegstra. 1997. Identification of protein transport complexes in the chloroplastic envelope membrane via crosslinking. *J. Cell Biol.* 136:983–994.
- Bauer, J., K. Chen, A. Hiltbrunner, E. Wherli, M. Eugster, D. Schnell, and F. Kessler. 2000. The major protein import receptor of plastids is essential for chloroplast biogenesis. *Nature.* 403:203–207.
- Bolhuis, A., J.E. Mathers, J.D. Thomas, C.M. Barrett, and C. Robinson. 2001. TatB and TatC form a functional and structural unit of the twin-arginine translocase from *Escherichia coli*. *J. Biol. Chem.* 276:20213–20219.
- Bölter, B., T. May, and J. Soll. 1998. A protein import receptor in pea chloroplasts, Toc86, is only a proteolytic fragment of a larger polypeptide. *FEBS Lett.* 441:59–62.
- Bölter, B., J. Soll, K. Hill, R. Hemmler, and R. Wagner. 1999. A rectifying ATP-regulated solute channel in the chloroplastic outer envelope from pea. *EMBO J.* 18:5505–5516.
- Bruce, B.D. 2001. The paradox of plastid transit sequences: conservation of function despite divergence in primary structure. *Biochim. Biophys. Acta.* 1541:2–21.
- Caliebe, A., R. Grimm, G. Kaiser, J. Lübeck, J. Soll, and L. Heins. 1997. The chloroplastic protein import machinery contains a Rieske-type iron-sulfur cluster and a mononuclear iron-binding protein. *EMBO J.* 16:7342–7350.
- Chen, K., X. Chen, and D.J. Schnell. 2000. Initial binding of preproteins involving the Toc159 receptor can be bypassed during protein import into chloroplasts. *Plant Physiol.* 122:813–822.
- Collinson, I., C. Breyton, F. Doung, C. Tziatzios, D. Schubert, E. Or, T. Rapoport, and W. Kühlbrandt. 2001. Projection structure and oligomeric properties of a bacterial core translocase. *EMBO J.* 20:2462–2471.
- Dorne, A.J., J. Joyard, M.A. Block, and R. Douce. 1985. Localization of phosphatidylcholine in outer envelope membrane of spinach chloroplast. *J. Cell Biol.* 100:1690–1697.
- Heins, L., A. Mehrle, R. Hemmler, R. Wagner, M. Küchler, D. Sveshnikov, and J. Soll. 2002. The preprotein conducting channel at the inner envelope membrane of plastids. *EMBO J.* 21:2616–2625.
- Hiltbrunner, A., J. Bauer, P.A. Vidi, S. Infanger, P. Weibel, M. Hohwy, and F. Kessler. 2001a. Targeting of an abundant cytosolic form of the protein import receptor atToc159 to the outer chloroplast membrane. *J. Cell Biol.* 154:309–316.
- Hiltbrunner, A., J. Bauer, M. Alvarez-Huerta, and F. Kessler. 2001b. Protein translocase at the Arabidopsis outer chloroplast membrane. *Biochem. Cell Biol.* 79:629–635.
- Hinnah, S.C., K. Hill, R. Wagner, T. Schlicher, and J. Soll. 1997. Reconstitution of a chloroplast protein import channel. *EMBO J.* 16:7351–7360.
- Hinnah, S.C., R. Wagner, N. Sveshnikova, R. Harrer, and J. Soll. 2002. The chloroplast protein import channel toc75: pore properties and interaction with transit peptides. *Biophys. J.* 83:899–911.
- Hirsch, S., E. Muckel, F. Heemeyer, G. von Heijne, and J. Soll. 1994. A receptor component of the chloroplast protein translocation machinery. *Science.* 266:1989–1992.
- Jarvis, P., L.J. Chen, H. Li, C.A. Peto, C. Fankhauser, and J. Chory. 1998. An Arabidopsis mutant defective in the plastid general protein import apparatus. *Science.* 282:100–103.
- Jelic, M., N. Sveshnikova, M. Motzkus, P. Hörth, J. Soll, and E. Schleiff. 2002. The chloroplast import receptor Toc34 functions as preprotein regulated GTPase. *Biol. Chem.* 383:1875–1883.
- Keegstra, K., and K. Cline. 1999. Protein import and routing systems of chloroplasts. *Plant Cell.* 11:557–570.
- Kerber, B., and J. Soll. 1992. Transfer of a chloroplast-bound precursor protein into the translocation apparatus is impaired after phospholipase C treatment. *FEBS Lett.* 306:71–74.
- Kessler, F., and G. Blobel. 1996. Interaction of the protein import and folding machineries of the chloroplast. *Proc. Natl. Acad. Sci. USA.* 93:7684–7689.
- Kessler, F., G. Blobel, H.A. Patel, and D.J. Schnell. 1994. Identification of two GTP-binding proteins in the chloroplast protein import machinery. *Science.* 266:1035–1039.
- Kouranov, A., X. Chen, B. Fuks, and D.J. Schnell. 1998. Tic20 and Tic22 are new components of the protein import apparatus at the chloroplast inner envelope membrane. *J. Cell Biol.* 143:991–1002.
- Küchler, M., and J. Soll. 2001. From nuclear genes to chloroplast localized proteins. *Plant Sci.* 161:379–389.
- Küchler, M., S. Decker, F. Hörmann, J. Soll, and L. Heins. 2002. Protein import into chloroplasts involves redox-regulated proteins. *EMBO J.* 15:6136–6145.
- Kunkele, K.P., S. Heins, M. Dembowski, F.E. Nargang, R. Benz, M. Thieffry, J. Walz, R. Lill, S. Nussberger, and W. Neupert. 1998. The preprotein translocation channel of the outer membrane of mitochondria. *Cell.* 93:1009–1019.
- Ma, Y., A. Kouranov, S.E. LaSala, and D.J. Schnell. 1996. Two components of the chloroplast protein import apparatus, IAP86 and IAP75, interact with the transit sequence during the recognition and translocation of precursor proteins at the outer envelope. *J. Cell Biol.* 134:315–327.
- Manting, E.H., C. van Der Does, H. Remigy, A. Engel, and A.J.M. Driessen. 2000. SecYEG assembles into a tetramer to form the active protein translocation channel. *EMBO J.* 19:852–861.
- Marabini, R., and J.M. Carazo. 1994. Pattern recognition and classification of images of biological macromolecules using artificial neural networks. *Biophys. J.* 66:1804–1814.
- Marabini, R., I.M. Masegosa, M.C. San Martiácuten, S. Marco, J.J. Fernaacutendez, L.G. de la Farga, C. Vaquerizo, and J.M. Carazo. 1996. XMIPP: an image processing package for electron microscopy. *J. Struct. Biol.* 116:237–240.
- Marco, S., M. Chagoyen, L.G. Delafraga, J.M. Carazo, and J.L. Carrascosa. 1996a. A variant to the “Random Approximation” of the reference-free alignment

- algorithm. *Ultramicroscopy*. 66:5–10.
- Marco, S., J.J. Fernandez, L.G. De La Fraga, C. Vaquerizo, and J.M. Carazo, J.M. 1996b. An image processing package for electron microscopy. *J. Struct. Biol.* 116: 237–240.
- May, T., and J. Soll. 2000. 14-3-3 proteins form a guidance complex with chloroplast precursor proteins in plants. *Plant Cell*. 12:53–63.
- Model, K., C. Meisinger, T. Prinz, N. Wiedemann, K.N. Truscott, N. Pfanner, and M.T. Ryan. 2001. Multistep assembly of the protein import channel of the mitochondrial outer membrane. *Nat. Struct. Biol.* 8:361–370.
- Nielsen, E., M. Akita, J. Davila-Aponte, and K. Keegstra. 1997. Stable association of chloroplastic precursors with protein translocation complexes that contain proteins from both envelope membranes and a stromal hsp100 molecular chaperone. *EMBO J.* 16:935–946.
- Pascual-Montano, A., L.E. Donate, M. Valle, M. Barcena, R.D. Pascual-Marqui, and J.M. Carazo. 2001. A novel neural network technique for analysis and classification of EM single-particle images. *J. Struct. Biol.* 133:233–245.
- Perry, S.E., and K. Keegstra. 1994. Envelope membrane proteins that interact with chloroplastic precursor proteins. *Plant Cell*. 6:93–105.
- Pohlmeyer, K., J. Soll, R. Grimm, K. Hill, and R. Wagner. 1998. A high-conductance solute channel in the chloroplastic outer envelope from pea. *Plant Cell*. 10:1207–1216.
- Pohlmeyer, K., J. Soll, T. Steinkamp, S. Hinnah, and R. Wagner. 1997. Isolation and characterization of an amino acid-selective channel protein present in the chloroplastic outer envelope membrane. *Proc. Natl. Acad. Sci. USA*. 94: 9504–9509.
- Radermacher, M. 1994. Three-dimensional reconstruction from random projections: orientational alignment via Radon transforms. *Ultramicroscopy*. 53: 121–136.
- Radermacher, M., T. Ruiz, H. Wiczkorek, and G. Gruber. 2001. The structure of the V(1)-ATPase determined by three-dimensional electron microscopy of single particles. *J. Struct. Biol.* 135:26–37.
- Sargent, F., U. Gohlke, E. de Leew, N.R. Stanley, T. Palmer, H.R. Saibil, and C. Berks. 2001. Purified components of the *Escherichia coli* tat protein transport system form a double-layered ring structure. *Eur. J. Biochem.* 268: 3361–3367.
- Schleiff, E., and J. Soll. 2000. Travelling of proteins through membranes: translocation into chloroplasts. *Planta*. 211:449–456.
- Schleiff, E., and R.B. Klösgen. 2001. Without a little help of “my” friends—direct insertion of proteins into chloroplast membranes? *Biochim. Biophys. Acta*. 1541:22–33.
- Schleiff, E., R. Tien, M. Salomon, and J. Soll. 2001. Lipid composition of outer leaflet of chloroplast outer envelope determines topology of OEP7. *Mol. Biol. Cell*. 12:4090–4102.
- Schleiff, E., J. Soll, N. Sveshnikova, R. Tien, S. Wright, C. Dabney-Smith, C. Subramanian, and B.D. Bruce. 2002a. Structural and GTP/GDP requirements for transit peptide recognition by the cytosolic domain of the chloroplast outer envelope receptor, Toc34. *Biochem.* 41:1934–1946.
- Schleiff, E., M. Motzkus, and J. Soll. 2002b. Chloroplast protein import inhibition by a soluble factor from wheat germ lysate. *Plant Mol. Biol.* 50:177–185.
- Schleiff, E., L.A. Eichacker, K. Eckart, T. Becker, O. Mirus, T. Stahl, and J. Soll. 2003. Prediction of the plant  $\beta$ -barrel proteome: a case study of the chloroplast outer envelope. *Prot. Sci.* In press.
- Schnell, D.J., F. Kessler, and G. Blobel. 1994. Isolation of components of the chloroplast protein import machinery. *Science*. 266:1007–1012.
- Schnell, D., G. Blobel, K. Keegstra, F. Kessler, K. Ko, and J. Soll. 1997. A consensus nomenclature for the protein-import components of the chloroplast envelope. *Trends Cell Biol.* 7:303–304.
- Seedorf, M., K. Waegemann, and J. Soll. 1995. A constituent of the chloroplast import complex represents a new type of GTP-binding protein. *Plant J.* 7:401–411.
- Sohrt, K., and J. Soll. 2000. Toc64, a new component of the protein translocator of chloroplast. *J. Cell Biol.* 148:1213–1221.
- Stahl, T., C. Glockmann, J. Soll, and L. Heins. 1999. Tic40, a new “old” subunit of the chloroplast protein import translocator. *J. Biol. Chem.* 274:37467–37472.
- Stoops, J.K., S.J. Kolodziej, J.P. Schroeter, J.P. Bretaudiere, and S.J. Wakil. 1992. Structure-function relationships of the yeast fatty acid synthase: negative-stain, cryo-electron microscopy, and image analysis studies of the end views of the structure. *Proc. Natl. Acad. Sci. USA*. 89:6585–6589.
- Sun, Y.-J., F. Forouhar, H.m. Li, S.-L. Tu, Y.-H. Yeh, S. Kao, H.-L. Shr, C.-C. Chou, C. Chen, and C.-D. Hsiao. 2002. Crystal structure of pea Toc34, a novel GTPase of the chloroplast protein translocator. *Nature Struct. Biol.* 9:95–100.
- Sveshnikova, N., R. Grimm, J. Soll, and E. Schleiff. 2000a. Topology studies of the chloroplast protein import channel Toc75. *Biol. Chem.* 381:687–693.
- Sveshnikova, N., J. Soll, and E. Schleiff. 2000b. Toc34 is a preprotein receptor regulated by GTP and phosphorylation. *Proc. Natl. Acad. Sci. USA*. 97:4973–4978.
- Tyedmers, J., M. Lerner, C. Bies, J. Dudek, M.H. Skowronek, I.G. Hass, N. Heim, J. Nastainczyk, J. Volkmer, and R. Zimmermann. 2000. Homologs of the yeast Sec complex subunits Sec62p and Sec63p are abundant proteins in dog pancreas microsomes. *Proc. Natl. Acad. Sci. USA*. 97:7214–7219.
- Van Heel, M. 1987. Similarity measures between images. *Ultramicroscopy*. 21:95–100.
- van Heel, M., and G. Harauz. 1988. Biological macromolecules explored by pattern recognition. *Scanning Microsc. Suppl.* 2:295–301.
- Waegemann, K., and J. Soll. 1991. Characterization of the protein import apparatus in isolated outer envelopes of chloroplasts. *Plant J.* 1:149–158.
- Waegemann, K., S. Eichacker, and J. Soll. 1992. Outer envelope membranes from chloroplasts are isolated as right-side-out vesicles. *Planta*. 187:89–94.